Self-Diffusion and Viscoelasticity of Linear Polystyrene in Entangled Solutions

Norio Nemoto,* Masahiro Kishine, Tadashi Inoue, and Kunihiro Osaki

Institute for Chemical Research, Kyoto University, Uji, Kyoto-fu 611, Japan

Received July 27, 1990; Revised Manuscript Received September 25, 1990

ABSTRACT: The slow chain dynamics of macromolecules in entangled solutions was studied from measurements of three characteristic quantities, the self-diffusion coefficient, D_s, the steady viscosity, η, and the steady-state compliance, J_e°, of linear polystyrene (PS) samples in 13, 18, and 40.6 wt % PS-dibutyl phthalate (DBP) solutions. The molecular weight, M, ranged from 43 900 to 5480 000. The product $D_s\eta/C$ was close to the theoretical prediction based on the free Rouse chain model at $M/M_e \sim 1$ and, for $M/M_e > 10$, showed universal behavior characterized by the linear proportionality to M/M_e. In the intermediate region of $1 < M/M_e < 10$, the dependence was found to be more complicated. Consistency between self-diffusion behavior and viscoelastic behavior was further examined in terms of the characteristic time for diffusion, $\tau_D = R_G^2/D_s$ (R_G: the unperturbed radius of gyration), and the corresponding time for viscoelasticity, $\tau_V = \eta J_e^\circ$. The ratio τ_V/τ_D took approximately a constant value of 0.15 ± 0.05 over the whole range of M/M_e studied, which is intermediate between respective theoretical values of the free Rouse chain model and the tube model, $^1/_{15}$ and $^1/_4$. The reduced plot of $D_s(M)/D_s(M_e)$ vs M/M_e was successful in superposition of the D_s data onto one master curve, which gave −2.5 as the exponent for $M/M_e > 10$. D_s data of PS solutions in different solvents as well as those of PS melts in the literature could be superposed onto our master curve in the range $0.5 < M/M_e < 10$ by using the same reduction procedure. Deviations from the master curve were only observed for D_s melt data above $M/M_e = 10$.

Introduction

In a previous publication,[1] we dealt with the tracer diffusion coefficient, D_{tr}^∞, of a linear polystyrene (PS) chain in an entanglement network composed of a very high molecular weight PS matrix in dibutyl phthalate (DBP). We found that the effect of entanglements on D_{tr}^∞ was properly extracted from data analysis in terms of two parameters, the effective friction coefficient of a segment, ζ, and the molecular weight between entanglements, M_e, which is in harmony with the modern concept of entanglement dynamics.[18] The range of polymer concentrations, C, studied was from 13 to 40.6 wt % and that of molecular weights from 6100 to 2890 000. The analysis gave the following relationship for D_{tr}^∞

$$D_{tr}^\infty(M) = f_2'(C,T)g_2'(C,M) \quad (1)$$

$$f_2'(C,T) = K_2T/\zeta(C,T) \quad (2)$$

$$g_2'(C,M) = M^{-1\pm0.1}, \quad M < M_e$$
$$= M^{-1}(M/M_e)^{-1.5\pm0.1}, \quad M \geq M_e \quad (3)$$

Here K_2 is a constant. This two-parameter scheme was already shown to be quite useful for the interpretation of linear as well as nonlinear viscoelastic properties of entangled homogeneous polymer solutions.[2]

A similar reduction procedure was applied to the self-diffusion coefficient (D_s) data of PS–DBP solutions at C = 40.6 wt % and those of PS melts.[3] In the reduced plot of $D_s(M)/D_s(M_e)$ vs M/M_e, we found that agreement between the two sets of data was satisfactory up to M/M_e = 10. For $M/M_e > 10$, however, the melt behavior of $D_s \propto M^{-2}$, which is significantly different from the solution behavior of $D_s \propto M^{-2.6\pm0.2}$, resulted in the failure of the two-parameter scheme. Such a difference in the exponents is in contrast to the steady viscosity (η) of PS, for which the 3.4 ± 0.1 power law holds for both the concentrated solution and the melt in the entangled state. The effect of entanglements in homogeneous polymeric systems thus looks more complicated.

Viscoelastic properties in the terminal zone can be characterized by the steady viscosity (η) and the steady-state compliance (J_e°), or its product, and the characteristic time, $\tau_V = \eta J_e^\circ$.[4] We may define $\tau_D = R_G^2/D_s$ as the corresponding characteristic time for the self-diffusion of a polymer molecule following the theory of Brownian motion. Here R_G is the radius of gyration. This expression implicitly assumes that the diffusant loses its initial memory in both the unentangled and the entangled state after times corresponding to the movement of the polymer center of mass by a distance R_G. Such an assumption is not a priori obviously true as was argued by Fixman.[27] Provided that the viscoelastic behavior and the self-diffusion behavior are dominated by the same slowest chain motion, however, we may expect that τ_V and τ_D are proportional to each other. We already observed that the product, $D_s\eta/C$, of the concentrated PS–DBP solutions became proportional to M/M_e for $M/M_e > 10$, i.e., in the highly entangled region.[3] Since $R_G^2 \propto M$ in the concentrated region and J_e° is independent of M and may be proportional to M_e/C for $M/M_e > 10$, the above observation is consistent with the expectation of $\tau_V/\tau_D = D_s\eta J_e^\circ/R_G^2$ = constant. Nevertheless, more direct evidence is clearly needed to obtain an umambiguous conclusion. Apart from the appreciable difference in M dependence of D_s between solution and melt, it seems worth examining the above expectation for simultaneous measurements of self-diffusion and viscoelasticity in the terminal zone of PS–DBP solutions at different C.

In this study, we report the results of forced Rayleigh scattering measurements and viscoelastic measurements on PS–DBP solutions at $C \simeq$ 13 and 18 wt % over a wide range of M. It will be shown that suitable data reduction, following the two-parameter scheme, makes it possible to construct one master curve on which our D_s data as well as those of PS in different solvents reported by other researchers are located.[5-7] Furthermore, consistency between self-diffusion and viscoelastic behavior is discussed in detail from dependences of $D_s\eta/C$ and τ_V/τ_D on M/M_e.

0024-9297/91/2224-1648$02.50/0

Table I
Characteristics of Polystyrene

code	$M_w/10^4$	M_w/M_n	code	$M_w/10^4$	M_w/M_n
F4	4.39	1.01	F80	77.5	1.01
F10	10.2	1.02	F128	126	1.05
F20	18.6	1.07	F288	289	1.09
F40	35.5	1.02	F550	548	1.15

Experimental Section

Materials. Eight samples of narrow distribution polystyrenes (TOSO) with different molecular weights were used in this study. Their sample codes, weight-average molecular weights (M_w), and ratios M_w/M_n are listed in Table I. The samples were labeled with a photobleachable dye of 2-nitro-4-carboxy-4'-(dimethylamino)stilbene following the labeling procedure described in an earlier paper.[8] GPC combined with low-angle light scattering measurements showed that there was no change in either molecular weight or molecular weight distribution of the polymers during the labeling procedure. Distilled dibutyl phthalate was used as a solvent.

Test solutions were prepared with exactly the same method described in ref 3. For viscoelastic measurements, eight solutions of unlabeled PSs listed in Table I with polymer concentration C = 13 wt % and two solutions of unlabeled F10 and F288 with C = 18 wt % were prepared. For forced Rayleigh scattering measurements, 1–5 wt % labeled PS was mixed into unlabeled PS of the same molecular weight, and two series of PS-DBP solutions with total concentrations of 13 and 18 wt % were prepared.

Methods. Forced Rayleigh scattering measurements were performed with an instrument described elsewhere.[9] Monochromatic light from an Ar ion laser (λ = 488 nm) and from a He–Ne laser (λ = 633 nm) was used as a writing and a reading beam, respectively. Acquisition and analysis of light intensity data, $I_d(t)$, diffracted from the solution were handled with a newly made processor. Measurements were made at 30 ± 0.05 °C on all solutions.

Time profiles of $I_d(t)$ could be fitted by eq 4 with a single decay rate (Γ_d) to all solutions. Here A is the amplitude, and B_1

$$I_d(t) = \{A \exp(-\Gamma_d t) + B_1\}^2 + B_2^2 \quad (4)$$

and B_2 are contributions from the coherent and the incoherent background optical field, respectively. Γ_d was estimated from a least-squares fit to an accuracy of 10%. D_s of the polymers in solution was calculated as the slope in the linear plot of Γ_d against the square of the wave vector $\mathbf{q}$, which is related to the grating spacing (d) as $|\mathbf{q}| = 2\pi/d$. Examples of such a plot are shown in earlier papers.[1,10]

Dynamic viscoelastic measurements were performed with an cone-and-plate type rheometer (RPX 705, Iwamoto) on solutions of the three highest molecular weight PS samples (F128, F288, and F550) and with a parallel-plate type rheometer (RMS 800, Rheometrix) on solutions of two PS samples (F40 and F80) over a range of frequency (ω) from 10^{-2} to 10^1 s^{-1}. Storage and loss shear moduli, $G'(\omega)$ and $G''(\omega)$, measured at temperatures from 0 to 60 °C were reduced to the reference temperature of 30 °C following the frequency–temperature superposition principle. The steady viscosity (η) was also measured on solutions of the three lower molecular weight samples (F4, F10, and F20) at 30 °C. To solutions of the three highest molecular weight samples, stress relaxation measurements were made to study their viscoelastic behavior in the terminal zone.

Results

Self-Diffusion Behavior. Figure 1 shows the dependence of the self-diffusion coefficient (D_s) of two series of PS–DBP solutions with C = 13 and 18 wt % on molecular weight in the range from 43 900 to 5480 000. Table II lists values of D_s at T = 30 °C. As a measure of the strength of entanglement coupling, the position of M_e on the abscissa is indicated by an arrow to each concentration in the figure. Here M_e was estimated from the empirical equation,[11] eq

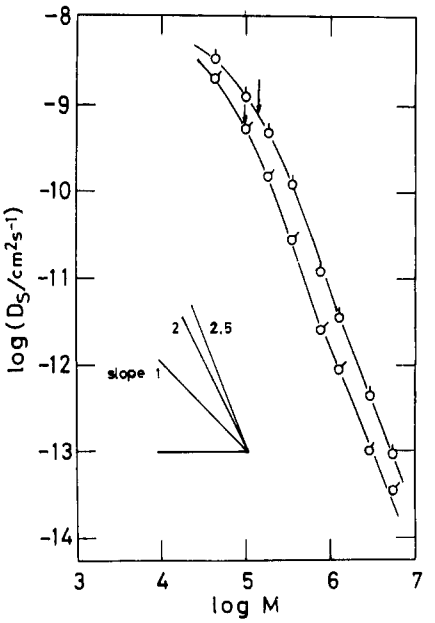

Figure 1. Self-diffusion coefficient, D_s, of 13 and 18 wt % PS–DBP solutions at 30 °C plotted against molecular weight, M. Symbols: (○) 13 and (○) 18 wt %. An arrow indicates the value of M_e at each concentration calculated from eq 5. The curves are empirically drawn for guidance of eye.

Table II
Values of D_s, η, and J_e° of PS–DBP Solutions at T = 30 °C

sample	C/wt %	$D_s/10^{-11}$ cm^2 s^{-1}	$\eta/10^2$ P	$J_e^\circ/10^{-4}$ cm^2 dyn^{-1}
F4	13	330	0.018	
F10	13	120	0.057	
F20	13	50	0.13	
F40	13	11	0.51	0.65
F80	13	1.1	4.6	1.2
F128	13	0.36	17	1.8
F288	13	0.045	530	1.9
F550	13	0.0089	4400	1.8
F4	18	200		
F10	18	53	0.11	
F20	18	16		
F40	18	3.1		
F80	18	0.25		
F128	18	0.09		
F288	18	0.01	4300	0.87
F550	18	0.0035		

5, whose applicability was extensively discussed in an

$$M_e = 1.8 \times 10^4 C^{-1} \quad (\mathrm{g/cm^3})^{-1} \quad (5)$$

earlier study.[1,33] The M_e values estimated are 130 000 and 96 000 at C = 13 and 18 wt %, respectively. In Figure 1, each solid curve is empirically drawn to respective concentrations for guidance of eye. The dependence of D_s on M is stronger than $D_s \propto M^{-1}$, predicted by the free Rouse chain model theory over the whole M range studied, and the curves may be approximately represented by the power law type equation at high molecular weights.

$$D_s \propto M^{-\alpha}, \quad \alpha = 2.5 \quad (6)$$

The same exponent, 2.5, was found for the tracer diffusion behavior of the same PS–DBP system for which the tracer diffusion coefficient (D_{tr}^∞) accurately obeyed $D_{tr}^\infty \propto M^{-2.5}$ above $M = M_e$. It is to be noted that if D_s data of 18 wt % solutions above $M = M_e$ were fitted by the power law with the least-squares method, a slightly higher exponent of 2.6 would be obtained. The whole aspect of M dependence of D_s at these relatively low C values is quite

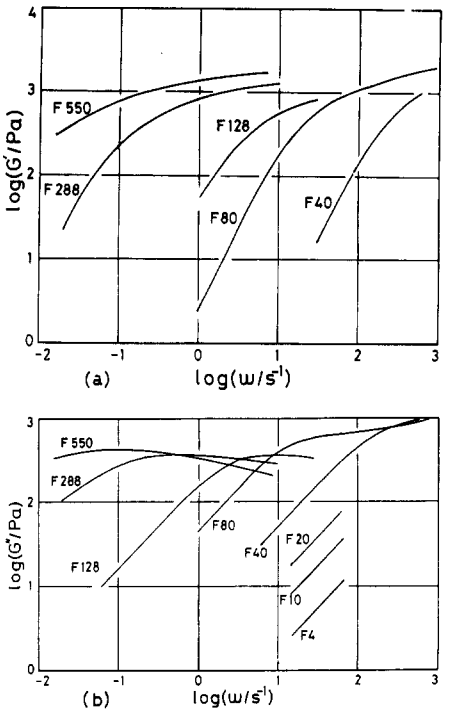

Figure 2. Complex shear modulus, G^*, of 13 wt % PS–DBP solutions at 30 °C. (a) Storage modulus, G', as a function of angular frequency, ω; (b) loss modulus, G'', vs ω.

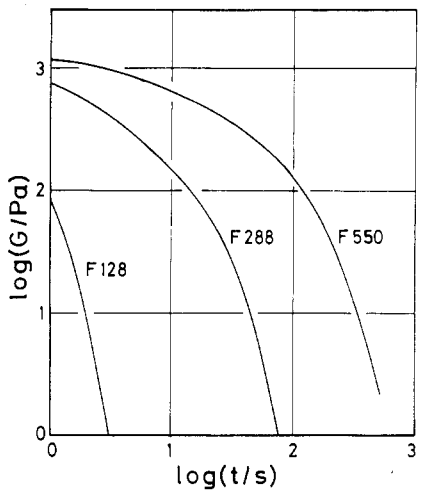

Figure 3. Shear relaxation modulus, $G(t)$, of 13 wt % PS–DBP solutions at 30 °C.

similar to that observed for the 40.6 wt % PS–DBP solution. Therefore, we may expect that suitable data reduction makes it possible to obtain one master curve, as will be shown later.

Viscoelastic Behavior. Figure 2 shows frequency dependences of the storage and loss moduli, $G'(\omega)$ and $G''(\omega)$, of five PS–DBP solutions from F40 to F550 at C = 13 wt %. For the three lowest molecular weight solutions from F4 to F20, we obtained only steady flow behavior, which is represented by the straight line with the slope of unity of the G'' vs ω plot. Since dynamical measurements on solutions of a few higher molecular weight PS samples were not conducted at a sufficiently low frequency region where $G'(\omega)$ becomes proportional to ω^2, shear stress relaxation moduli, $G(t)$, of the three solutions F128, F288, and F550 were measured as shown in Figure 3. The values of $G(t)$ obtained were in good agreement with those calculated from the dynamic complex modulus, $G^*(\omega)$, by applying an approximate interconversion formula.[4] The

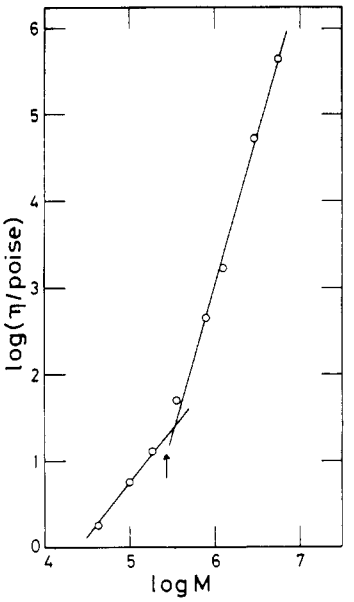

Figure 4. Steady viscosity, η, of 13 wt % PS–DBP solutions at 30 °C plotted against molecular weight, M. An arrow indicates the value of $2M_e$.

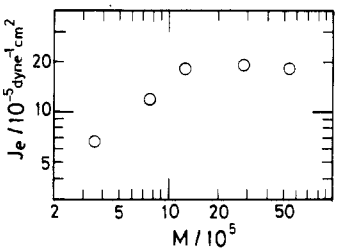

Figure 5. Steady compliance, $J_e°$, of 13 wt % PS–DBP solutions at 30 °C plotted against molecular weight, M.

relaxation moduli of Figure 3 were well-represented by a sum of exponential functions. Stretched exponential functions with a cut-off at long times may also be fitted. The steady viscosity (η) and the steady compliance ($J_e°$) were estimated from the curves in Figures 2 and 3. The values of η and $J_e°$ are given in Table II. The η and $J_e°$ values of the 13 wt % PS–DBP solutions are logarithmically plotted against M in Figures 4 and 5, respectively. The dependence of η on M may be represented by two straight lines with the slope 1.2 ± 0.1 at lower molecular weights and 3.5 ± 0.1 at higher molecular weights. The molecular weight, M_c, at the break point is about equal to twice M_e, as is shown by the arrow in the figure. In the entangled state, $J_e°$ first increases with M and then becomes independent of M above $M \sim 10M_e$. It is well-known that $\eta \propto M^{3.5\pm0.1}$ and $J_e \propto M^0$ are characteristic of the viscoelastic behavior of highly entangled monodisperse polymers in the flow region.[4,12] Our PS–DBP system exhibits this characteristic feature above $M/M_e = 10$, which is slightly larger than values of 3–6 observed for other polymer solutions and melts.

Characteristic Time for Diffusion and Viscoelasticity. We here take $\tau_D = R_G^2/D_s$ and $\tau_V = \eta J_e°$ as the characteristic time for diffusion and viscoelasticity, respectively. For calculation of τ_D, we employed the R_G–M_w relationship at the Θ state.[13]

$$R_G^2 = 7.86 \times 10^{-18} M_w \qquad (7)$$

Equation 7 may be applicable for R_G of PS in the melt but may not be used for accurate estimate of R_G of PS in a good solvent at finite concentration where chain expansion due to the excluded volume and chain contraction due to

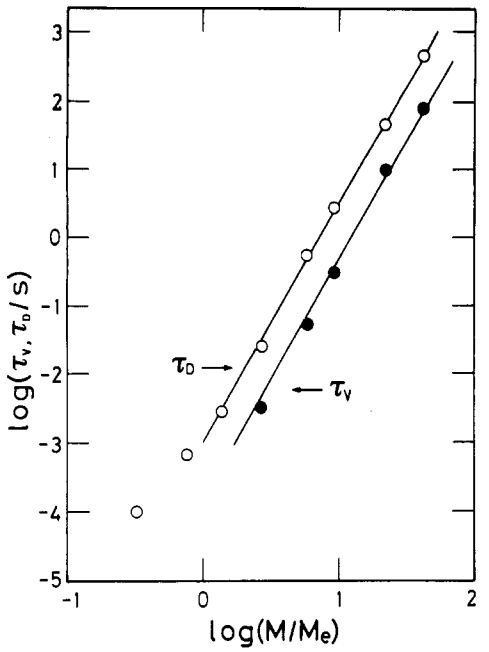

Figure 6. Characteristic times for diffusion and viscoelasticity, $\tau_D = R_G^2/D_s$ and $\tau_V = \eta J_e^\circ$, of 13 wt % PS-DBP solutions plotted against the number of entanglements per chain, M/M_e.

concentration screening are competing. However, a linear relationship of R_G^2 to M_w was confirmed by Daoud et al. from small-angle neutron-scattering measurements on PS-CS_2 solutions over a wide range of concentration.[14] Therefore, the use of eq 7 as an approximate estimate of R_G may not lead to an erroneous conclusion in discussing the M dependence of τ_D at fixed C.

Figure 6 gives a plot of τ_D and τ_V against the number of entanglement couplings per chain M/M_e. Since J_e° could not be measured for low molecular weight PS samples, τ_V was calculated only for entangled polymer solutions. Both quantities appear to increase in parallel to each other with increasing M/M_e with the same slope of 3.5 ± 0.1. These data are the first clear-cut demonstration that slow chain dynamics caused by random thermal fluctuation and slow chain relaxation observed by application of mechanical force are dominated by the same molecular mechanism in entangled solutions. It may be noted that proportionality of τ_V to τ_D does not hold for entangled PS melts owing to $D_s \propto M^{-2}$ and $\eta \propto M^{3.5}$ at the high molecular weight end. Comparison of the ratio τ_V/τ_D with theoretical predictions will be made later.

Discussion

Consistency between Self-Diffusion and Viscoelasticity. The quantities D_s and η both contain a parameter, ζ, whose magnitude is unknown. Their product, $D_s\eta$, however, does not depend on ζ, because $D_s \propto \zeta^{-1}$ and $\eta \propto \zeta$.[3,10,15] Therefore, $D_s\eta$ can be directly compared with theories without any adjustable parameter. Here we have chosen two theories for comparison with our data; one is the Rouse theory[4,16] developed for unentangled polymer chain dynamics in concentrated solution and melt, and the other the Doi-Edwards (DE) theory[17,18] for highly entangled chain dynamics. The Rouse theory predicts

$$D_s\eta/C = RTR_G^2/6M \quad (8)$$

indicating that $D_s\eta/C$ is a constant independent of C and M, if R_G^2 is proportional to M. The tube model theory predicts that $D_s\eta/C$ should be linearly proportional to

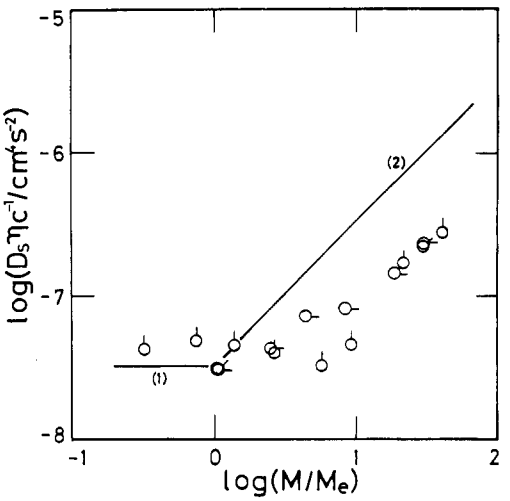

Figure 7. Product of the viscosity and the self-diffusion coefficient divided by concentration plotted against M/M_e. Symbols: (○) 13, (◐) 18, and (◑) 40.6 wt %. Lines 1 and 2 are predictions of eqs 8 and 9, respectively.

M/M_e in the entangled state.

$$D_s\eta/C = (RTR_G^2/6M)(M/M_e) \quad (9)$$

Theoretical predictions of eqs 8 and 9, lines 1 and 2, respectively, are compared with values of $D_s\eta/C$ estimated for the PS-DBP solutions at three concentrations of 13, 18, and 40.6 wt % in Figure 7. Here we used eq 7 for an estimate of R_G^2, neglecting its C dependence.[19] The data are fairly in agreement with the Rouse theoretical value in the unentangled region of $M/M_e < 1$. In the range of $M/M_e > 10$, all data points obtained at different C values appear to converge to one straight line with a slope of about unity. The slope agrees with the theoretical prediction, line 2 of the tube model theory. However, the absolute magnitude given by the theory is about 5 times larger than the experimental values. In the lightly entangled region of $1 < M/M_e < 10$, there seems to be no trend, as is readily seen from the figure, for the data to show the systematic dependence on M/M_e. Thus, we arrive at the conclusion that universality concerning C and M dependences of $D_s\eta/C$ is attained in the highly entangled state of polymer molecules.

We showed in the previous section that the characteristic times for diffusion and viscoelasticity, τ_D and τ_V, both increase with the same molecular weight exponent of 3.5 with increasing M. If the self-diffusion and viscoelastic behavior of entangled polymer solutions are governed by the same molecular motion mechanism, we may expect that the ratio τ_V/τ_D takes a constant value independent of either C or M. In order to examine this, we reanalyzed complex shear modulus data of 40.6 wt % DBP solutions of four PS samples (F10, F20, F40, and F80) used for evaluation of η in the earlier publication[1] and estimated J_e° and subsequently, τ_V/τ_D. The ratio τ_V/τ_D thus obtained is plotted against M/M_e with those of 13 and 18 wt % solutions in Figure 8. The data look pretty scattered at first glance, but this data scattering may be ascribed to experimental uncertainties involved in the ratio that is evaluated from three independent observables, D_s, η, and J_e^0, and also R_G calculated from eq 7. Thus, we tentatively propose that the ratio approximately takes a constant value of 0.15 ± 0.05 over the whole range of M/M_e studied.

$$\tau_V/\tau_D = \eta J_e^\circ D_s/R_G^2 = 0.15 \pm 0.05 \quad (10)$$

The Rouse theory and the DE theory predict $^1/_{15}$ and $^1/_4$ as the values of τ_V/τ_D, respectively. The experimental

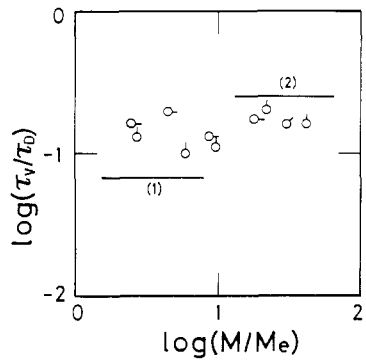

Figure 8. Ratio τ_V/τ_D plotted against M/M_e. Symbols are the same as in Figure 7. Lines 1 and 2 are predictions of the Rouse and Doi–Edwards theories, respectively.

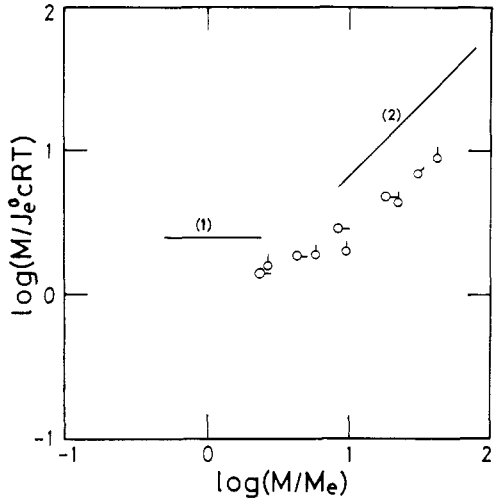

Figure 9. Reduced steady compliance, $M/J_e^\circ CRT$, plotted against M/M_e. Symbols are the same as in Figure 7. Lines 1 and 2 are predictions of eqs 11 and 12, respectively.

value is intermediate between them.

Figure 9 shows the double-logarithmic plot of reduced steady compliance $M/J_e^\circ CRT$ against M/M_e. Line 1 in the figure is the theoretical prediction to a free Rouse chain.

$$M/J_e^\circ CRT = 2.5 \tag{11}$$

Straight line 2 with a slope of unity is the prediction to a chain making curvilinear motion through the tube.

$$M/J_e^\circ CRT = 2M/3M_e \tag{12}$$

We could not confirm the validity of eq 11 because of a lack of data in the unentangled state. In the entangled state, the reduced compliance remains constant or slightly increases up to $M/M_e \sim 10$ where the value becomes close to the Rouse value of 2.5, and then it begins to increase almost linearly with increasing M/M_e. The universal behavior with a slope of unity for $M/M_e > 10$ qualitatively agrees with the prediction of the DE theory. Quantitatively, the theory underestimates J_e° by a factor of about 3. It may be noted that C and M dependences of J_e° are qualitatively predictable from corresponding dependences of $D_s\eta/C$ in Figure 7 and the proportionality relation to τ_V to τ_D, eq 10. Modification of the latter gives

$$D_s\eta/C \propto (R_G^2/M)(M/J_e^\circ CRT) \tag{13}$$

If R_G^2 is proportional to M, $D_s\eta/C$ and $M/J_e^\circ CRT$ are expected to exhibit similar C and M dependences. Comparison of Figures 7 and 9 shows that the expectation is roughly satisfied in the entangled region. The results

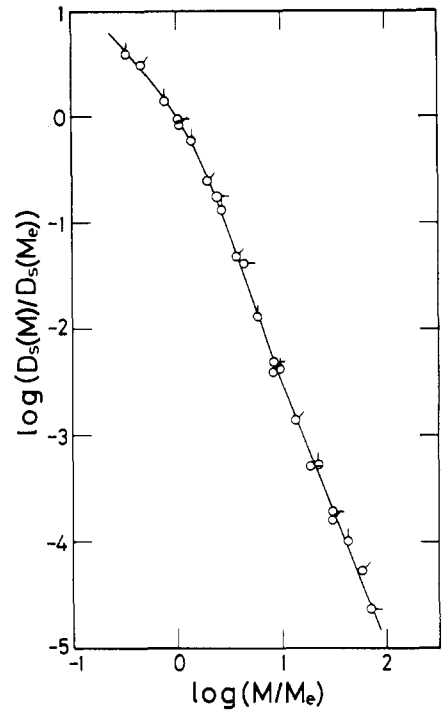

Figure 10. Reduced self-diffusion coefficient data, $D_s(M)/D_s(M_e)$, plotted against M/M_e. Symbols are the same as in Figure 7. The solid curve is the master curve that most closely represents the reduced D_s data.

presented in Figures 7–9 clearly demonstrate that D_s, η, and J_e° are closely interrelated to one another through eq 10, which after all reduces to presence of the single relaxation time intrinsic of respective polymer–solvent systems. Stated in another way, one physically plausible model is sufficient to interprete self-diffusion behavior and viscoelastic behavior of entangled homogeneous polymer solutions simultaneously.

Reduction of D_s Data. The self-diffusion coefficient can be expressed by the product of two separate contributions, f_2 and g_2, f_2 from microBrownian motion of a segment and g_2 from the effect of the topological interaction with surrounding chains. The function f_2 may be inversely proportional to a segment friction coefficient ζ, which depends on C and is independent of the polymer molecular weight at high M. Since the lowest molecular weight of the PS samples used in this study is 43 900, the dependence of ζ on M is negligible. By taking a ratio of two D_s values at different molecular weights at the same C, we may eliminate the function f_2 containing ζ of unknown magnitude. Invoking that the viscoelasticity of entangled polymeric systems is characterized by two parameters, ζ and M_e, we adopt a value of D_s at M_e as the reference value for reduction. The value of $D_s(M_e)$ at each C is easily estimated from the respective curves given in Figure 1 by interpolation. The retardation effect on self-diffusion of a polymer chain due to the surrounding matrix may be scaled by the mesh size of the entanglement network corresponding to M_e, dependent on only C or, equivalently, by the number of entanglements per chain, M/M_e. The reduced self-diffusion coefficient, $D_s(M)/D_s(M_e)$, at $C = 13$ and 18 wt %, and also at 40.6 wt % reported in an earlier paper,[3] is plotted against M/M_e in Figure 10. As is evident from the figure, superposition looks quite satisfactory over the whole range of M/M_e from 0.3 to 70 studied, indicating the success of the two-parameter scheme. The master curve thus obtained appears to be represented above $M/M_e = 10$ by the straight line with a slope of −2.5, which agrees with M dependence of reduced

D_{tr}^∞ data of the same polymer–solvent system. This agreement strongly suggests that the power law of $D_s \propto M^{-2.5}$ is universal to D_s of PS solutions in the highly entangled solution state.

The following remark to the shape of the master curve in the figure seems helpful. The master curve of the reduced D_{tr}^∞ in the range of M/M_e from 0.05 to 30 was represented by two straight lines intersecting at $M \sim M_e$ as given by eqs 1–3. On the other hand, the master curve of the reduced D_s neither shows a sharp break at $M \sim M_e$ nor allows the approximation by one straight line above M/M_e. When the straight line at high M/M_e values is extrapolated to the low M/M_e region, D_s values in the range $1 < M/M_e < 10$ deviate upward from the line. Enhancement in D_s values at weak strength of entanglement coupling in comparison with the D_{tr}^∞ behavior may be one of the noticeable features of the self-diffusion in which the probe chain and the matrix chains have the same characteristic time for diffusion. Indeed D_s values are always larger than D_{tr}^∞ even at the highest M/M_e values studied, which seems to persist up to extremely high molecular weights. It may be inferred that a gradual increase in J_e° with M/M_e in the range from 1 to 10 is closely related to the self-diffusion behavior in the same M/M_e range in such a manner to satisfy eq 10. However, we do not pursue this problem further here, because small polydispersity in the samples possibly affects J_e° and D_s to some extent but probably with different weights.

The exponent $\alpha = 2.5$ at high M/M_e appears appreciably larger than those obtained for D_s of PS samples in different solvents in the similar concentration range. Leger et al.[5] gave 2 as the exponent for D_s of PS in benzene at $C = 10$ and 20 wt %, and Wesson et al.[6] reported the same value of 2 to the PS–THF system in the C range from 10 to 30 wt %. In a study by Callaghan and Pinder on D_s of PS in carbon tetrachloride and deuteriobenzene,[7] they observed an increase in the exponent with increasing C and found 2–2.1 in the C range from 0.095 to 0.20 g/cm^3. All of those data were obtained at relatively low molecular weights, i.e., in the M/M_e range from 0.5 to 8. Since the self-diffusion behavior is more complicated in the crossover region of $1 < M/M_e < 10$, the discrepancy of the exponent between our data and their D_s data might be only apparent. In order to show this and also to examine the validity of the two-parameter scheme, their $D_s(M)$ data were reduced by employing $D_s(M_e)$ directly read from respective figures given in their papers and are plotted against M/M_e in Figure 11. Here we used eq 5 for an estimate of M_e for all solutions, assuming that variation in M_e due to the difference in solvent power for PS is negligibly small.[20] The solid curve in the figure is the master curve of our reduced D_s data reproduced from Figure 10. Original data points were omitted for clarity of the figure. In the figure, we also gave the reduced self-diffusion data of PS melts for comparison. As is seen from the figure, reduced D_s values of various PS–solvent systems are not only superposed to one another but also are fairly well located on our master curve. As a matter of fact, the latter agreement is partly due to the shape of the master curve concave to the abscissa in the crossover region. Thus, we are led to the conclusion that if the power law were applied to D_s obtained in the limited range of relatively low M/M_e values, the exponent might be evaluated as about 2.0 ± 0.1, and with a further increase in M/M_e, it asymptotically approaches 2.5, characteristic of a highly entangled network.

The above conclusion appears, at present, applicable only for entangled PS solutions. PS melt data are in

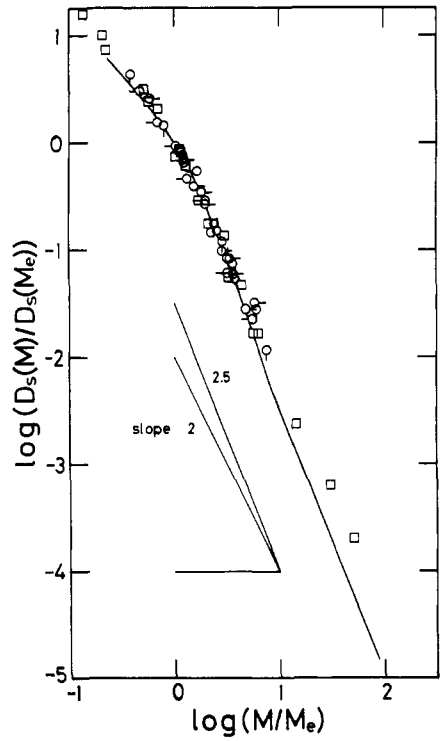

Figure 11. Reduced D_s data of PS in various solvents[5-7] plotted against M/M_e. Symbols: (○) PS in CCl_4 at $C = 0.20$ g/cm^3; (○-) PS in d-Bz at $C = 0.095$ and 0.175 g/cm^3;[7] (○) PS in Bz at $C = 10$ and 20 wt %;[5] (-○) PS in THF at $C = 10$ and 20 wt %.[6] The solid curve is the master curve reproduced from Figure 10. The reduced D_s data (□) of PS in melts are also reproduced from Figure 7 of ref 3 for comparison.

excellent agreement with the solution data up to $M/M_e = 10$, but they exhibit a significant deviation from the master curve for $M/M_e > 10$. We already showed consistency between self-diffusion behavior and viscoelastic behavior in entangled polymer solutions in the previous section. On the other hand, inconsistent results of $\eta \propto M^{3.5}$ and $D_s \propto M^{-2}$ are reported for PS melts, and various ideas have been put forward to explain it. The inverse square proportionality of D_s to M in melts has been found for other polymer species such as hydrogenated polybutadiene[21] and also polyethylene[22] in the highly entangled region. The exception has been reported for polyisoprene melt to which the exponent 2.5–2.8 is observed as M exceeds 100 000, i.e., for $M/M_e > 10$.[23] Thus, the question still remains as to whether the exponent 2 is universally applicable to any polymer melt.

We are now at the stage to make brief remarks to recent theoretical advances in slow polymer chain dynamics. It is well-known that the original DE theory based on the tube model[17,18] predicts $D_s \propto M^{-2}$ and $\eta \propto M^3$. In order to reconcile the latter prediction with the well-established experimental results of $\eta \propto M^{3.4\pm0.1}$, theoretical refinements or modifications were made without any alteration in M dependence of D_s.[24-28] A mode–mode coupling theory developed by Schweizer,[29] to be considered as the counterpart of the reptation theory, gives predictions on M dependences of D_s, η, and J_e° for the bulk polymer the same as the DE theory does. For entangled polymer solutions, however, the M dependence of D_s is affected by the excluded volume in such a way that the exponent has a little larger magnitude if chains are collapsed and has a smaller magnitude (<2) when the chains are expanded.[34] On the other hand, recent simulation works based on the cage model[30] and also on the repton model[31] predict $\eta \propto M^{3.4\pm0.1}$ and $D_s \propto M^{-2.5\pm0.1}$. It should be noted that both

models are essentially equivalent to the tube model, though slightly modified. Another formulation,[32] which semiempirically took into account memory effects arising from material inhomogeneity and cooperative molecular motion, predicts that the exponents for D_s and η should lie between $-7/3$ and $-37/15$ and between $10/3$ and $11/3$, respectively. A few among the theoretical predictions given above are in accordance with the results of our solution data. However, it seems too early to judge which model correctly catches the nature of slow molecular motion in entanglement network.

Acknowledgment. N.N. is greatly indebted to Dr. H. Watanabe of Osaka University for helpful discussions. We thank the Rheometrix people for their help in viscoelastic measurements on PS solutions. Thanks are also rendered to TOSO for supplies of PS samples.

References and Notes

(1) Nemoto, N.; Kishine, M.; Inoue, T.; Osaki, K. *Macromolecules* **1990**, *23*, 659.
(2) Osaki, K. In *Molecular Conformation and Dynamics of Macromolecules in Condensed Systems in Polymer Science*; Nagasawa, M., Ed.; Elsevier: Amsterdam, 1988; Vol. 2, pp 185–201.
(3) Nemoto, N.; Kojima, T.; Inoue, T.; Kishine, M.; Hirayama, T.; Kurata, M. *Macromolecules* **1989**, *22*, 3793.
(4) Ferry, J. D. *Viscoelastic Properties of Polymers*, 3rd ed.; John Wiley: New York, 1980.
(5) Leger, L.; Hervet, H.; Rondelez, F. *Macromolecules* **1981**, *14*, 1732.
(6) Wesson, J. A.; Noh, I.; Kitano, T.; Yu, H. *Macromolecules* **1984**, *17*, 782.
(7) Callaghan, P. T.; Pinder, D. *Macromolecules* **1984**, *17*, 431.
(8) Inoue, T.; Nemoto, N.; Kojima, T.; Kurata, M. *Polym. J.* **1988**, *20*, 869.
(9) Inoue, T.; Nemoto, N.; Kojima, T.; Kurata, M. *Nihon Reorji Gokkaishi* **1988**, *16*, 72 (in Japanese).
(10) Nemoto, N.; Kojima, T.; Inoue, T.; Kurata, M. *Polym. J.* **1988**, *20*, 875.
(11) Osaki, K.; Nishimura, Y.; Kurata, M. *Macromolecules* **1985**, *18*, 1153.
(12) Graessley, W. W. *Adv. Polym. Sci.* **1974**, *16*, 1.
(13) Fukuda, M.; Fukumoto, M.; Hashimoto, T. *J. Polym. Sci., Polym. Phys. Ed.* **1974**, *12*, 871.
(14) Daoud, M.; Cotton, J. P.; Farnoux, B.; Jannink, G.; Sarma, G.; Benoit, H.; Duplessix, R.; Picot, C.; de Gennes, P. G. *Macromolecules* **1975**, *8*, 804.
(15) Nemoto, N.; Landry, M. R.; Noh, I.; Yu, H. *Polym. Commun.* **1984**, *25*, 141.
(16) Rouse, P. E. *J. Chem. Phys.* **1953**, *21*, 1212.
(17) Doi, M.; Edwards, S. F. *J. Chem. Soc., Faraday Trans. 2* **1978**, *74*, 1789.
(18) Doi, M.; Edwards, S. F. *The Theory of Polymer Dynamics*; Clarendon Press: Oxford, 1986.
(19) The C dependence of R_G may be approximately estimated by referring to a work of King et al. (*Macromolecules* **1985**, *18*, 709). They reported that a PS chain expands in toluene by 18% as C decreases from 40 to 13 wt %. Since toluene is a better solvent than DBP to PS, correction of R_G due to the concentration effect is surely smaller than the estimated experimental error of 20%.
(20) As long as the mass density, g/cm^3, is used as the unit of C, eq 5 describes to a good approximation the M_e–C relation for most of the PS–solvent system, though quite empirically.
(21) Bartles, C. R.; Christ, B.; Graessley, W. W. *Macromolecules* **1984**, *17*, 2702.
(22) Pearson, D. S.; VerStrate, G.; von Meerwall, E.; Schilling, F. G. *Macromolecules* **1987**, *20*, 1133.
(23) Yu, H. In *Molecular Conformation and Dynamics of Macromolecules in Condensed Systems in Polymer Science*; Nagasawa, M., Ed.; Elsevier: Amsterdam, 1988; Vol. 2, pp 107–132.
(24) Graessley, W. W. *Adv. Polym. Sci.* **1982**, *47*, 67.
(25) Doi, M. *J. Polym. Sci., Polym. Lett. Ed.* **1981**, *19*, 265; *J. Polym. Sci., Polym. Phys. Ed.* **1983**, *21*, 667.
(26) Hess, W. *Macromolecules* **1986**, *19*, 1395; **1987**, *20*, 2587.
(27) Fixman, M. *J. Chem. Phys.* **1988**, *89*, 3892, 3912.
(28) Watanabe, H.; Tirrell, M. *Macromolecules* **1989**, *22*, 927.
(29) Schweizer, K. S. *J. Chem. Phys.* **1989**, *91*, 5802, 5822.
(30) Deutsch, J. M.; Madden, T. L. *J. Chem. Phys.* **1989**, *91*, 3252.
(31) Chang, I. S.; Rubinstein, M. *APS* **1990**, *35*, 456.
(32) Douglas, J. F. *Macromolecules*, submitted.
(33) For PS–aroclor solutions of $C < 10$ wt %, we found that the relation $M_e = 1.05 \times 10^4 C^{-1.3}$ gave a better fit to the experimental M_e–C curves. The M_e values at $C = 13$ and 18 wt % estimated from the above relation and eq 5 agreed with each other within an experimental uncertainty of 10%.
(34) Schweizer, K. S. Private communication.